Dominant formation and quenching kinetics of electron beam pumped Xe_2Cl

G. Marowsky

Max-Planck-Institut für Biophysikalische Chemie, Abteilung Laserphysik, D-3400 Göttingen, Federal Republic of Germany

G. P. Glass, M. Smayling, F. K. Tittel, and W. L. Wilson

Rice Quantum Institute, Chemistry and Electrical Engineering Departments, Rice University, Houston, Texas 77001

(Received 9 February 1981; accepted 15 April 1981)

Processes leading to the production and removal of the triatomic excimer Xe_2Cl^* subsequent to short duration electron beam excitation of $Ar/Xe/CCl_4$ mixtures have been investigated. The radiative lifetime of Xe_2Cl^* has been measured to be 135 $(^{+70}_{-60})$ ns. Formation of the excimer has been shown to occur principally via a termolecular reaction involving XeCl*. Rate constants for the formation and collisional quenching of Xe_2Cl^* by CCl_4, Xe, and Ar have been determined.

I. INTRODUCTION

There has been a considerable interest in triatomic excimers as media for tunable lasers in the visible and UV wavelength region for a variety of applications. Broadband continuous emission due to bound–free transitions of Rg_2X^* trimers has been observed from several electron beam excited high pressure rare gas–halide mixtures.[1–4] However, while the broadband nature of these transitions offers wavelength tunability, the effective gain of the triatomic excimers is low compared to that of the molecular diatomic excimers. To date two molecules (Xe_2Cl[5] and Kr_2F[6]) have demonstrated laser action centered at 520 and 436 nm, respectively. The stimulated emission occurs for transitions between bound ionic excited states and repulsive covalent lower states.[1] The bound–free nature of the laser transition prevents population buildup in the lower laser level. The kinetics of these lasers is not completely understood for electron beam excited rare gas–halide mixtures. However, kinetic studies of Xe_2Cl and Kr_2F using synchrotron radiation excitation and photolytic pumping have recently been reported.[7–10] In this paper we discuss the formation and quenching kinetics of Xe_2Cl^* based on fluorescence studies of high pressure $Ar/Xe/CCl_4$ mixtures irradiated by short duration electron beam pulses. This information can be used to evaluate and predict the performance characteristics of the Xe_2Cl laser.

II. EXPERIMENTAL APPARATUS AND TECHNIQUES

In order to obtain the high pumping powers needed to achieve laser action of triatomic excimers, electron beam excitation was used to form excited buffer gas (argon) atoms and ions. These species, in turn, react with the rare gas and halogen donors to create the excimers. The experiments were carried out in a stainless steel cell attached to the field emission diode of an electron beam accelerator (Physics International Pulserad 110). A beam of 1 MeV electrons with a pulse duration of 10 ns (FWHM) was injected transversely into the reaction cell through a 50 μ thick titanium anode foil over an area of 1×10 cm, with a current density of ~ 100 A/cm^2 at the optical axis. Details of the apparatus have been reported previously in Ref. 11, and are shown in Fig. 1.

The rare gases used in these studies were of research grade, and were turbulently mixed. A considerable decrease of emission intensity was observed if successive shots were taken with the same mixture. In order to assure good shot to shot reproducibility, a fresh gas mixture was prepared for each measurement.

All of the measurements were made with computer aided instrumentation. Temporal behavior of both fluorescence and laser output was obtained with a fast photodiode (ITT F4000-S5), and recorded with a transient digitizer (Tektronix R7912). Interference/color glass filters defined the spectral region of interest. Simultaneously, time integrated, spectrally resolved data were recorded with a calibrated optical multichannel analyzer (PAR OMA1). Both the OMA and the

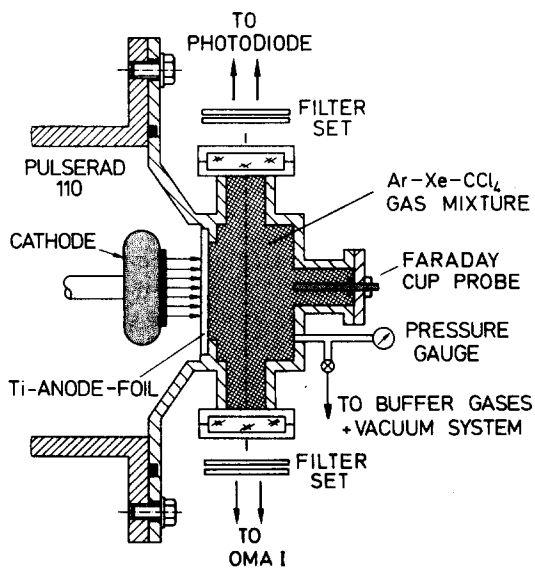

FIG. 1. Diagram of the electron beam pumped reaction cell.

 0021-9606/81/151153-06$01.00

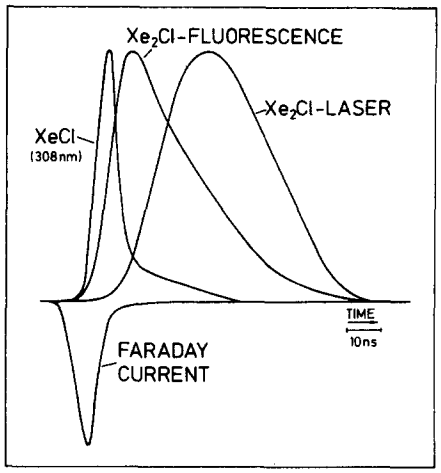

FIG. 2. Typical temporal characteristics of XeCl and Xe_2Cl fluorescence and laser pulses. The electron beam excitation pulse as monitored by a Faraday current probe is also indicated.

transient digitizer were interfaced to a DEC PDP 11/23 minicomputer system. Subsequent data reduction and feature extraction were accomplished with computer routines developed for these studies.

The temporal behavior of Xe_2Cl fluorescence and laser emission is shown in Fig. 2. This figure depicts the normalized, spectrally resolved photodiode signals of Xe_2Cl fluorescence and laser output at 500 nm. The fluorescence of XeCl ($B \rightarrow X$) at 308 nm and the electron beam pulse are also shown. An intracell resonator, consisting of two high reflectivity dielectric mirrors, was used in the laser experiments.[5]

A typical example of a time integrated fluorescence spectrum obtained with the OMA 1 is shown in Fig. 3. In the case of XeCl both an intense, narrow linewidth $B \rightarrow X$ transition and a broadband $C \rightarrow A$ transition are observed at 308 and 345 (± 20 nm), respectively. Xenon pressures in excess of 100 Torr favor the formation of Xe_2Cl^*. Figure 3 also depicts the broadband emission of this trimer centered close to 500 nm. The intensities shown are not correct for the spectral response of the OMA model 1205D/01 vidicon detector, for which the sensitivity (counts/photon) drops by a factor of 5 from 500 to 308 nm.

III. FORMATION MECHANISM AND KINETICS OF THE Xe_2Cl EXCIMER

Previous studies have shown that fluorescence originating from both $XeCl^*$ and Xe_2Cl^* is emitted when high density $Ar/Xe/CCl_4$ mixtures are excited by short duration pulses of 1 MeV electrons.[1,5,12] Emission from $XeCl^*$ precedes that from Xe_2Cl^*, and it has been suggested that $XeCl^*$ is a precursor in the reaction chain leading to the formation of Xe_2Cl^*.[7,13] In order to test this hypothesis, a model containing reactions for producing and removing Xe_2Cl^* was constructed, and its predictions were compared with experimental observations. The model contained the following reactions:

$$XeCl^* + Xe + Ar \rightarrow Xe_2Cl^* + Ar \ , \tag{1}$$

$$Xe_2Cl^* \rightarrow 2Xe + Cl + h\nu \ , \tag{2}$$

$$Xe_2Cl^* + CCl_4 \rightarrow \text{quenched product} + CCl_4 \ , \tag{3}$$

$$Xe_2Cl^* + Xe \rightarrow \text{quenched product} + Xe \ , \tag{4}$$

$$Xe_2Cl^* + Ar \rightarrow \text{quenched product} + Ar \ . \tag{5}$$

A termolecular reaction was selected for the formation of Xe_2Cl^* in order to keep the mechanism as simple as possible. This reaction is also the predominant formation mechanism for other Rg_2X^* species.[9,4,15] Preliminary experiments had shown that fluorescence from Xe_2Cl^* was enhanced relative to that from $XeCl^*$ when the partial pressures of both Xe and Ar were increased. Therefore, the formation mechanism should contain both Xe and Ar. Reactions (2)–(5) were selected to represent loss of Xe_2Cl^* by radiative decay and by collisions with various quenching gases.

The rate equation pertinent to the above mechanism can be written in the following form:

$$\frac{d}{dt}[Xe_2Cl^*] = k_1(XeCl^*)(Xe)(Ar) - \frac{(Xe_2Cl^*)}{\tau} \ , \tag{6}$$

where k_1 is the termolecular rate constant and τ is the effective exponential decay constant for Xe_2Cl^*, given by

$$\tau^{-1} = \tau_{500}^{-1} + k^q_{CCl_4}(CCl_4) + k^q_{Xe}(Xe) + k^q_{Ar}(Ar) \ . \tag{7}$$

Here τ_{500} is the radiative lifetime of Xe_2Cl^* which emits at 500 nm, and $k^q_{CCl_4}$, k^q_{Xe}, and k^q_{Ar} are rate constants for the quenching of Xe_2Cl^* by CCl_4, Xe, and Ar, respectively. In all of these expressions ( ) denotes particle density in cm^{-3}. Equation (6) can be converted to an expression containing I_{308} and I_{500}, the fluorescent intensities of $XeCl^*$ and Xe_2Cl^*, respectively, upon dividing the concentrations of $XeCl^*$ and Xe_2Cl^* by the appropriate radiative lifetimes. After rearranging, the following equation is obtained[16]:

$$\frac{d}{dt}(I_{500}) = k_1(Xe)(Ar)I_{308}\left(\frac{\tau_{308}}{\tau_{500}}\right) - \frac{I_{500}}{\tau} \ . \tag{8}$$

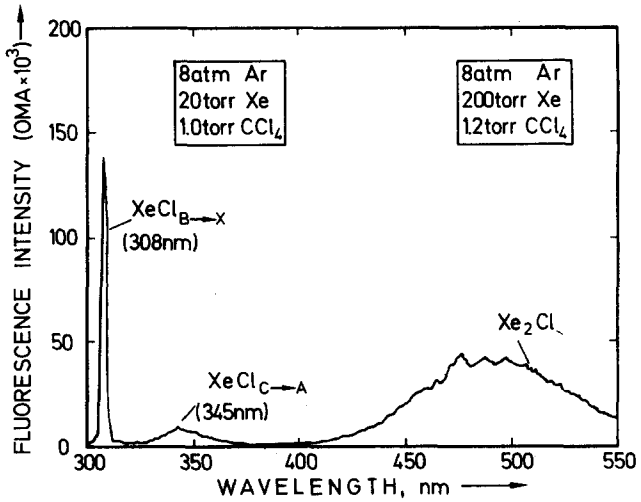

FIG. 3. Temporally integrated fluorescence spectrum of Xe_2Cl, XeCl ($B \rightarrow X$), and XeCl ($C \rightarrow A$).

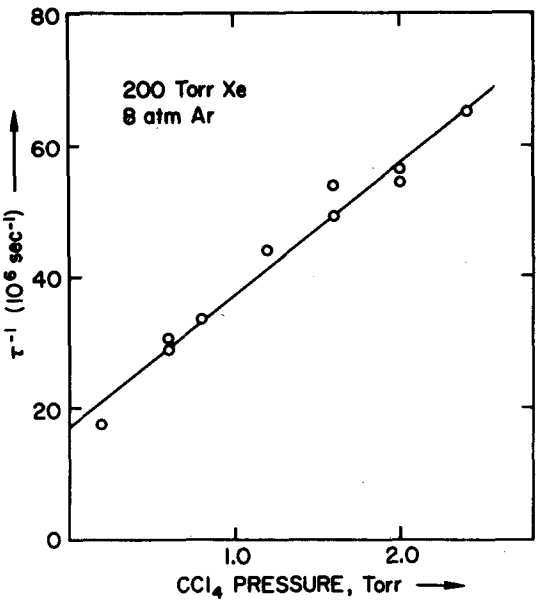

FIG. 4. The decay frequency of the Xe_2Cl^* fluorescence at 500 nm as a function of CCl_4 pressure for mixtures containing fixed amounts of argon and xenon.

IV. EXPERIMENTAL RESULTS

Under all conditions investigated, the fluorescence emitted by XeCl at 308 nm was observed to decay much more rapidly than that emitted at 500 nm by Xe_2Cl. Therefore, the effective decay constant τ for Xe_2Cl could be measured by monitoring I_{500} *after* I_{308} had effectively decayed to zero. This allowed quenching studies to be made that were independent of the precise details of the Xe_2Cl formation mechanism.

The rate of collisional quenching of Xe_2Cl^* by CCl_4 was established by measuring the decay constant τ for a number of mixtures containing constant amounts of Xe and Ar, but different amounts of CCl_4. Some of the experimental data are shown in Fig. 4. In this figure, the Xe_2Cl decay frequency τ is plotted as a function of the CCl_4 pressure for mixtures containing 200 Torr xenon and 8 atm argon. From the slope of Fig. 4, $k^q_{CCl_4}$ was calculated as $(6\pm1)\times10^{-10}$ cm^3 s^{-1}.

Collisional quenching of Xe_2Cl^* by Xe and by Ar was studied in a manner similar to that described above. A change in τ was observed when the partial pressure of argon was varied between 1 and 8 atm in mixtures containing fixed amounts of Xe and CCl_4. From these measurements, a value of $(3\pm1)\times10^{-14}$ cm^3 s^{-1} was estimated for k^q_{Ar}. An apparently systematic variation in τ was also observed when the partial pressure of Xe was varied from 50 to 400 Torr in mixtures containing 2 Torr of CCl_4 and 2 atom of argon. However, the magnitude of this variation was very small. Therefore, the value of 5×10^{-13} cm^3 s^{-1} estimated for k^q_{Xe} from these measurements should be regarded only as an upper limit for this rate constant.

The radiative lifetime of Xe_2Cl^* can be estimated from the zero pressure intercept in Fig. 4. This intercept contains contributions due to collisional quenching of Xe_2Cl^* by Xe and by Ar. However, when these were subtracted, as indicated by Eq. (7), $(\tau_{500})^{-1}$ was computed as $(7.5^{+6.5}_{-2.6})\times10^6$ s^{-1}. The error in this value arises in part from the scatter in the data shown in Fig. 4. However, the main contribution arises from the uncertainty in our knowledge of k^q_{Xe} and k^q_{Ar}. The magnitude of the error reflects the fact that, in all of the mixtures studied, Xe_2Cl^* was principally removed by collisions with CCl_4.

The Xe_2Cl formation mechanism was investigated by observing temporal fluorescence profiles using the fast photodiode and by recording the time-integrated spectrally resolved data taken by the optical multichannel analyzer. Qualitative predictions of the mechanism listed in the previous section were first verified; thereafter, calculations were performed in order to compare actual experimental data with quantitative predictions of the model.

Initially, Eq. (8) was used to analyze the temporal behavior of the fluorescence emitted by XeCl ($B\rightarrow X$) at 308 nm, and by Xe_2Cl at 500 nm. Values of I_{500} and I_{308} were monitored using the photodiode in successive identical experiments, and were compared when I_{500} reached a maximum. At that instant the lhs of Eq. (8) is equal to zero, and the equation can be rearranged to yield

$$\frac{I_{500}}{I_{308}} = k_1(\mathrm{Xe})\,(\mathrm{Ar})\,\tau\left(\frac{\tau_{308}}{\tau_{500}}\right) . \tag{9}$$

Two series of rare gas–halide mixtures were studied: one containing 2 Torr CCl_4, 2 atm Ar, and variable pressures of Xe ranging from 50 to 400 Torr, and another containing 2 Torr CCl_4, 8 atm Ar, and varying amounts of Xe ranging from 200 to 600 Torr. The effective decay constant τ for Xe_2Cl was measured in each experiment, and was found to be approximately constant, varying only by ± 12%. The ratio I_{500}/I_{308} was found to be linear in Xe partial pressure, and to be approximately four times greater in mixtures containing 8 atm Ar than in mixtures containing 2 atm argon.

In order to confirm this result based on temporal data, another series of experiments was performed. In these experiments, the total "time-integrated" fluorescence emitted throughout the experiment was measured using an optical multichannel analyzer (OMA). Using this device, time integrated fluorescence emitted by Xe_2Cl^* at 500 nm, i.e., $\int I_{500}\,dt$, could be compared in the same experiment to that emitted by $XeCl^*$ at 308 nm. The mechanism outlined in the previous section predicts that the total amount of Xe_2Cl^* formed per unit volume over the duration of the experiment is

$$k_1\int_0^\infty (\mathrm{XeCl}^*)\,(\mathrm{Xe})\,(\mathrm{Ar})\,dt , \tag{10}$$

which can be rewritten as

$$k_1(\mathrm{Xe})\,(\mathrm{Ar})\,\tau_{308}\int I_{308}\,dt . \tag{11}$$

The fraction of Xe_2Cl^* that emits radiation in the 500 nm band is (τ/τ_{500}). Therefore, the total number of photons emitted by Xe_2Cl^* in the 500 nm band throughout the experiment is

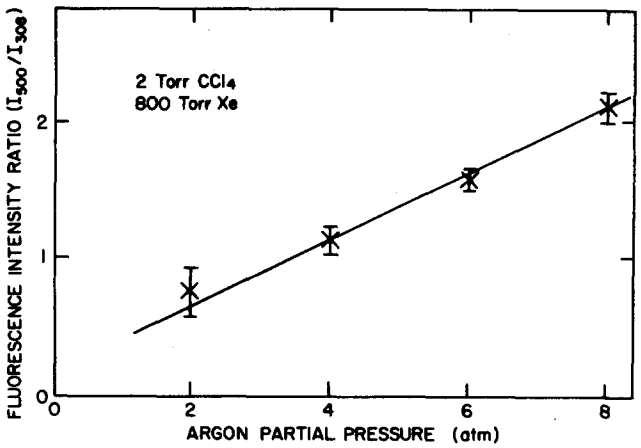

FIG. 5. The ratio of total fluorescence emitted by Xe_2Cl^* at 500 nm to that emitted by $XeCl^*$ at 308 nm plotted against argon pressure for mixtures containing a fixed amount of CCl_4 and Xe. Each plotted point represents an average of four to eight experimental measurements. The error bars represent the standard deviation of each set of measurements.

$$\int I_{500}\,dt = k_1(\mathrm{Xe})\,(\mathrm{Ar})\,\tau(\tau_{308}/\tau_{500})\int I_{308}\,dt\ . \qquad (12)$$

Thus, the fluorescence ratio ($\int I_{500}dt/\int I_{308}dt$) is predicted to be linear in the partial pressure of xenon and argon.

Figure 5 displays the experimentally measured fluorescence ratio ($\int I_{500}dt/\int I_{308}dt$) as a function of the argon partial pressure in mixtures containing 2 Torr CCl_4 and 800 Torr Xe. Using the value of τ obtained from the photodiode experiments, the measured value of 135 ns for τ_{500}, and an estimated value of 16 ns[7] for τ_{308}, k_1 was calculated from Eq. (12) as $(1.2\pm0.2)\times10^{-31}$ $cm^6\,s^{-1}$.

Figure 6 shows the variation of experimentally measured fluorescence ratio with xenon partial pressure. As can be seen, the ratio is linear in the partial pressure of xenon in mixtures containing both 8 atm argon and 2 atm argon. The constant k_1 was estimated from the slopes of Fig. 6 as $(1.5\pm0.1)\times10^{-31}$ $cm^6\,s^{-1}$ using the 8 atm mixtures and as $(1.6\pm0.2)\times10^{-31}$ $cm^6\,s^{-1}$ using the 2 atm mixtures.

The linearity of the fluorescence ratio with both xenon and argon and the near identity between the rate constant obtained from Figs. 5 and 6 provides strong evidence in favor of the proposed mechanism, although the slight nonzero intercept displayed by the 2 atm data may be statistically significant, and may represent a slight contribution from another Xe_2Cl^* source. Further evidence in support of the termolecular formation model was obtained by comparing the experimental Xe_2Cl fluorescence profile with that obtained by numerically integrating the rate equation pertinent to the proposed Xe_2Cl^* formation mechanism using Euler's method with a step size of $\sim4\times10^{-11}$ s. The concentration of $XeCl^*$ was calculated from the intensity of the experimentally measured XeCl ($B\rightarrow X$) fluorescence, and was used as input data into the calculation. The input took the form of an array of 512 successive intensity measurements recorded by the transient digitizer over a total time interval of 20 or 50 ns. The radiative lifetime of Xe_2Cl^* was taken as 135 ns, and the rate constants for the various quenching reactions were chosen as $k^q_{CCl_4}=6.0\times10^{-10}$ $cm^3\,s^{-1}$, $k^q_{Xe}=5.0\times10^{-13}$ $cm^3\,s^{-1}$, and $k^q_{Ar}=3.0\times10^{-14}$ $cm^3\,s^{-1}$ in order to fit the quenching data described previously. The termolecular rate constant k_1 was taken to be 1.5×10^{-31} $cm^6\,s^{-1}$. In order to better compare theory with experiment, the computed values were multiplied by a scaling factor in order to adjust the maximum of the computed I_{500} profile to that of the experimental one. This factor varied from 0.8 to 1.3. For comparison, it should be noted that the peak fluorescence measured in "identical" experiments varied by as much as 15%.

Temporal profiles of Xe_2Cl fluorescence were calculated using the postulated mechanism for a wide variety of CCl_4/Xe/Ar mixtures ranging from 2 Torr CCl_4, 50 Torr Xe, and 2 atm Ar, to 10 Torr CCl_4, 600 Torr Xe, and 8 atm Ar. Two comparisons between calculation and experiment are shown in Figs. 7(a) and 7(b). Equally good comparisons were obtained for all other mixtures studied, except for one, in which superradiance occurred in the XeCl ($B\rightarrow X$) transition, thus destroying the linear relationship between emission intensity and emitter concentration. The overall degree of agreement between calculation and experiment was excellent and strongly confirms the validity of the proposed Xe_2Cl^* formation mechanism.

V. CONCLUSIONS

In this paper fluorescence experiments have been described that reveal some of the details concerning the formation and quenching of the triatomic excimer Xe_2Cl^* which is produced by short duration electron beam pulse excitation of Ar/Xe/CCl_4 mixtures. It has been demonstrated that Xe_2Cl^* is formed primarily in a termolecular reaction involving the diatomic excimer

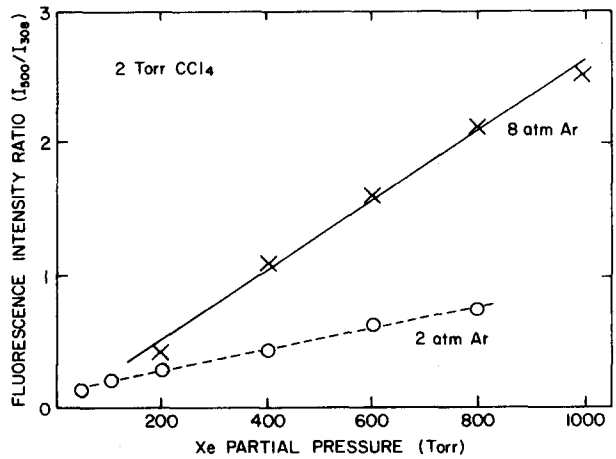

FIG. 6. The ratio of total fluorescence emitted at 500 nm to that emitted at 308 nm plotted as a function of Xe partial pressure. All measurements were made using mixtures containing 2 Torr CCl_4. The lower series of points refers to mixtures containing 2 atm Ar, the upper to mixtures with 8 atm of Ar.

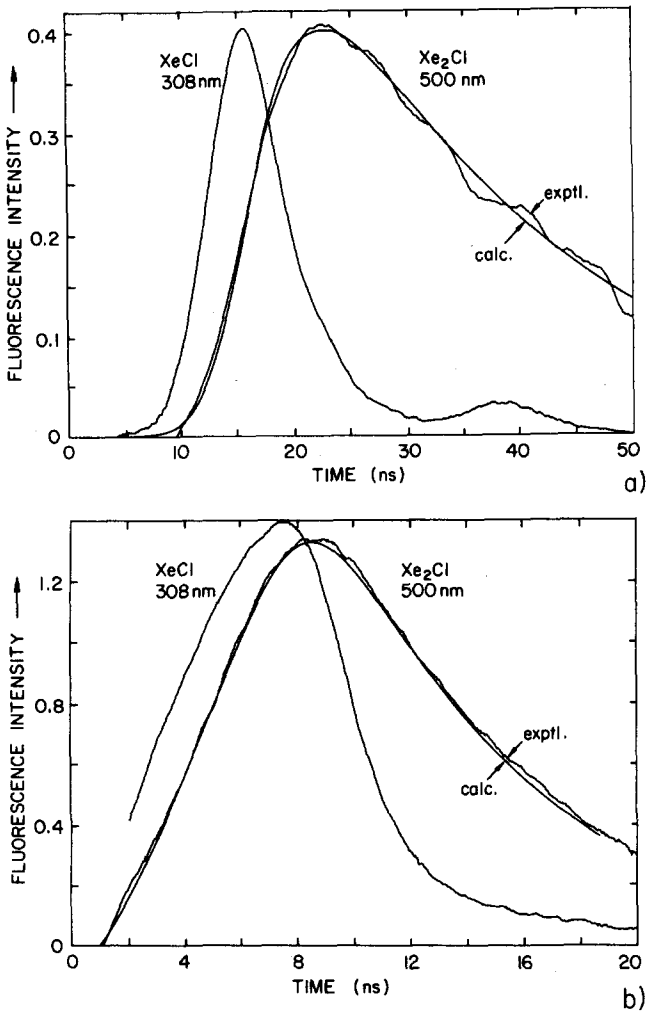

FIG. 7. Observed and calculated time dependence of XeCl ($B \rightarrow X$) and Xe_2Cl fluorescence (a) for a mixture of 2 atm Ar, 400 Torr Xe, 2 Torr CCl_4 and (b) 8 atm Ar, 600 Torr Xe, and 10 Torr CCl_4.

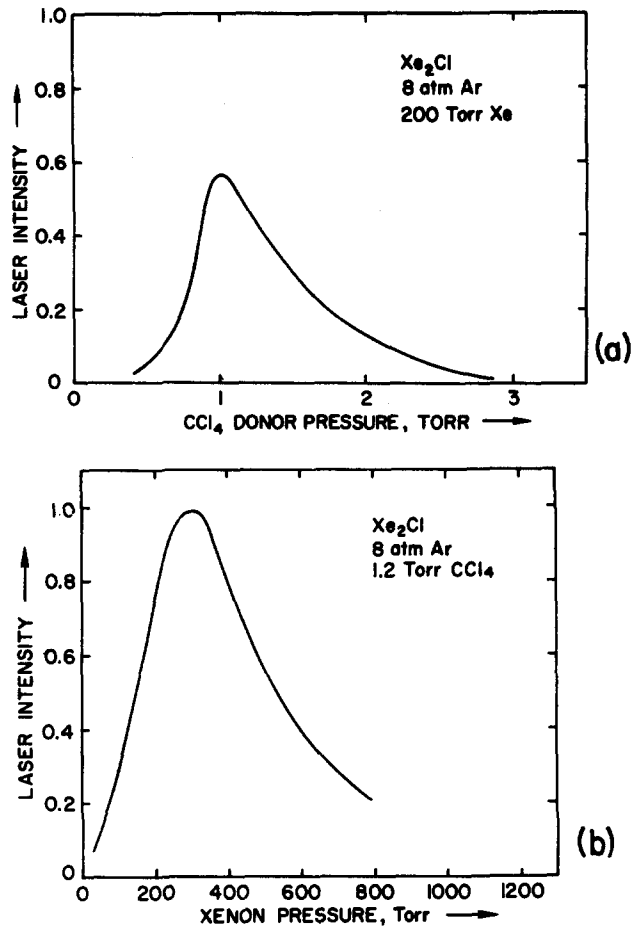

FIG. 8. Laser intensity as a function of CCl_4 halogen donor pressure and xenon pressure. The intracell resonator consisted of a spherical end reflector ($r = 1$ m, $R > 99\%$) and a flat output coupler ($R = 98\%$) spaced 10 cm apart.

$XeCl^*$. Rate constants for the formation reaction and for several bimolecular quenching reactions of Xe_2Cl^* have been measured. In addition, the radiative lifetime of Xe_2Cl^* has been estimated. A summary of these rate constants is given in Table I. The rate constants and radiative lifetime determined in Refs. 8 and 10 are consistent with the values determined in this work. The data of Tang *et al.* and Grieneisen *et al.* support a value for the radiative lifetime of Xe_2Cl^* of 210 ± 20 and 185 ± 10 ns, respectively.

It is clear, on the basis of the results presented in Table I, that quenching by CCl_4 is the dominant loss process in the Xe_2Cl laser system. Quenching by argon and by xenon is less severe. Quenching conditions play an important role in determining laser operating characteristics. This fact is well illustrated in Fig. 8. As

TABLE I. Summary of Xe_2Cl^* rate constants.

Reaction	Rate constant	Other work
(1) $XeCl^* + Ar + Xe \rightarrow Xe_2Cl^* + Ar$	k_1 (Ar, Xe) $= (1.5 \pm 0.5) \times 10^{-31}$ cm^6 s^{-1}	7.3×10^{-31} cm^6 s^{-1} for Xe buffer[a]
(2) $Xe_2Cl^* \rightarrow 2Xe + Cl + h\nu$ (500 nm)	$\tau_{500} = 135\ (+70-60)$ ns	120 ns,[b] 210 ns,[a] 185 ns[c]
(3) $Xe_2Cl^* + CCl_4 \rightarrow$ Quenching	$k^q_{CCl_4} = (6 \pm 1) \times 10^{-10}$ cm^3 s^{-1}	5×10^{-10} cm^3 s^{-1} for Cl_2,[a] 2.6×10^{-10} cm^3 s^{-1} [c]
(4) $Xe_2Cl^* + Ar \rightarrow$ Quenching	$k^q_{Ar} = (3 \pm 1) \times 10^{-14}$ cm^3 s^{-1}	
(5) $Xe_2Cl^* + Xe \rightarrow$ Quenching	$k^q_{Xe} < 5 \times 10^{-13}$ cm^3 s^{-1}	$< 4 \times 10^{-14}$ cm^3 s^{-1},[a] 6×10^{-15} cm^3 s^{-1} [c]

[a]Reference 8.
[b]Reference 12.
[c]Reference 10.

can be seen, the effective pressure range for CCl_4 and xenon in this system is limited. Two alternate halogen donors (Cl_2 and HCl) were found to inhibit laser action in the present experimental arrangement.

The postulated mechanism predicts a very high efficiency for production of Xe_2Cl^* from $XeCl^*$. The production efficiency increases at high argon pressures, reaching a value of 60% at 15 atm argon. To date, however, the laser output power has been limited by the presence of transient molecular and atomic absorptions induced by electron beam pumping.[5,6] The delayed appearance of the Xe_2Cl laser output shown in Fig. 2 is caused by the initial transient argon buffer gas absorption.[17] In addition, atomic absorptions from xenon metastables to Rydberg states lead to considerable reduction of the laser output.

ACKNOWLEDGMENTS

The authors would like to acknowledge the experimental assistance of Z. Guo. This research was supported jointly by the Office of Naval Research, the National Science Foundation, and the Robert A. Welch Foundation.

[1]D. C. Lorents, D. L. Huestis, G. V. McCusker, H. H. Nakano, and R. M. Hill, J. Chem. Phys. 68, 4657 (1978).
[2]J. A. Mangano, J. H. Jacob, M. Rokni, and A. Hawryluk, Appl. Phys. Lett. 31, 26 (1977).
[3]N. G. Basov, V. A. Danilychev, V. A. Dolgikh, O. M. Karimov, V. S. Lebedev, and A. G. Molchanov, JETP Lett. 26, 16 (1977).
[4]J. G. Eden, R. S. F. Chang, and L. J. Palumbo, IEEE J. Quantum Electron. 15, 1146 (1979).
[5]F. K. Tittel, W. L. Wilson, R. E. Stickel, G. Marowsky, and W. E. Ernst, Appl. Phys. Lett. 36, 405 (1980).
[6]F. K. Tittel, M. Smayling, W. L. Wilson, and G. Marowsky, Appl. Phys. Lett. 37, 862 (1980).
[7]D. L. Huestis, R. M. Hill, D. J. Eckstrom, M. V. McCusker, D. C. Lorents, H. H. Nakano, B. E. Perry, and N. E. Schlotter, "New Electronic Transition Laser Systems," SRI Technical Report I, May 1978.
[8]K. Y. Tang, D. C. Lorents, R. L. Sharpless, D. L. Huestis, D. Helms, M. Durrett, and G. K. Walters, 33rd Gaseous Electronics Conference, Norman, OK, 8 October 1980; also "Lasers '80," New Orleans, 19 December 1980.
[9]G. P. Quigley and W. M. Hughes, Appl. Phys. Lett. 32, 649 (1978).
[10]H. P. Grieneisen, H. Xue-Ting, and K. L. Kompa, Chem. Phys. Lett. (to be published).
[11]G. Marowsky, R. Cordray, F. K. Tittel, and W. L. Wilson, Appl. Opt. 17, 3491 (1978).
[12]K. Y. Tang, D. C. Lorents, and D. L. Huestis, Appl. Phys. Lett. 36, 347 (1980).
[13]K. Y. Tang, D. C. Lorents, and D. L. Huestis, 32nd Gaseous Electronics Conference, Pittsburgh, 9–12 October 1979.
[14]D. L. Huestis, Topical Meeting on Excimer Lasers, Charleston, S. C., 11–13 September 1979.
[15]M. Rokni, J. H. Jacob, and J. A. Mangano, Phys. Rev. A 16, 2216 (1977).
[16]In the interest of brevity, I has been expressed as a photon flux. Conversion to an energy flux requires multiplication by the photon energy $h\nu$.
[17]E. Zamir, D. L. Huestis, H. H. Nakano, R. M. Hill, and D. L. Lorents, IEEE J. Quantum Electron. 15, 281 (1979).